

Accepted Manuscript

Ice morphology modification and solute recovery improvement by heating and annealing during block freeze-concentration of coffee extracts

C.M. Robles, M.X. Quintanilla-Carvajal, F.L. Moreno, E. Hernández, M. Raventós, Y. Ruiz



PII: S0260-8774(16)30192-3

DOI: [10.1016/j.jfoodeng.2016.05.021](https://doi.org/10.1016/j.jfoodeng.2016.05.021)

Reference: JFOE 8574

To appear in: *Journal of Food Engineering*

Received Date: 26 October 2015

Revised Date: 17 May 2016

Accepted Date: 23 May 2016

Please cite this article as: Robles, C.M., Quintanilla-Carvajal, M.X., Moreno, F.L., Hernández, E., Raventós, M., Ruiz, Y., Ice morphology modification and solute recovery improvement by heating and annealing during block freeze-concentration of coffee extracts, *Journal of Food Engineering* (2016), doi: 10.1016/j.jfoodeng.2016.05.021.

This is a PDF file of an unedited manuscript that has been accepted for publication. As a service to our customers we are providing this early version of the manuscript. The manuscript will undergo copyediting, typesetting, and review of the resulting proof before it is published in its final form. Please note that during the production process errors may be discovered which could affect the content, and all legal disclaimers that apply to the journal pertain.

Ice morphology modification and solute recovery improvement by heating and annealing during block freeze-concentration of coffee extracts

Robles C.M.^a, Quintanilla-Carvajal M.X.^a, Moreno F.L.^a, Hernández E.^b, Raventós M.^b, Ruiz Y.^{a*}

^a Agro-industrial Process Engineering, Universidad de La Sabana, Campus Universitario del Puente del Común, km 7 Autopista Norte de Bogotá, Chía, Cundinamarca, Colombia

^b Agri-Food Engineering and Biotechnology Department, Universidad Politécnica de Cataluña (UPC), C/EsteveTerradas, 8, 08860 Castelldefels, Barcelona, Spain

*Corresponding author. Tel.: +57 1 8615555x25217.

e-mail address: ruth.ruiz@unisabana.edu.co (Y. Ruiz).

Abstract

Several treatments on ice blocks can be applied during block freeze-concentration to increase the solute recovery from the ice. In the present study, the changes in the ice block's temperature and the application of annealing during the block freeze-concentration of aqueous coffee extracts were studied. The ice block was subjected to heating and annealing prior to the thawing stage. The effect of coolant temperature during ice block heating ($T = -10$ and -5°C) and the application of annealing (+, -) on solute recovery and ice structure morphology was evaluated. The use of annealing during block freeze-concentration modified the ice crystal morphology and increased the solute recovery only when it is applied at the highest temperature. In general, the annealing process increased the size and circularity of the ice crystals, consequently improving the solute recovery. Thus, annealing can be used to increase the solute recovery during block freeze-concentration.

1 Introduction

In the food industry, products must often be concentrated to increase their shelf life as well as to decrease their transportation and processing costs. This concentration is required for freeze-dried soluble coffee production in which water must be removed from the coffee extract to increase the solids content and to decrease the time and cost of drying (Moreno et al., 2014b). Freeze-dried coffee is a higher quality product compared with spray-dried coffee because of the low temperatures used during processing (Fissore et al., 2014). Consequently, water removal should be performed at low temperatures (Moreno et al., 2015a; Van Pelt & Bassoli, 1990), which requires that freeze-concentration must be accomplished prior to freeze-drying.

Freeze-concentration (FC) is a technology used to partially remove water from coffee extracts. FC is known for its ability to preserve the organoleptic quality and functional properties of food solutions (Moreno et al., 2015a). Water removal during freeze-concentration is achieved by cooling the product of interest to form ice crystals in the solution, which are later removed (Belén

et al., 2012; Sánchez et al., 2009). Three techniques are used for freeze concentration: suspension FC, film FC (falling-film FC or progressive FC) and block FC (freezing-thawing-concentration). Suspension freeze concentration is the process used at the industrial level. This method involves forming many ice crystals in a scraped-surface heat exchanger. Then, these ice crystals are grown in a stirred crystallizer tank until they reach an appropriate size that can then be separated in a wash column. Suspension freeze concentration is an effective method but has a high investment cost. Therefore, other techniques, such as falling-film freeze concentration and block freeze concentration, have been studied to decrease investment and operating costs (Miyawaki et al., 2005; Sánchez et al., 2009).

Falling-film freeze concentration requires the formation of a single crystal that grows layer-by-layer on the solution, while block freeze concentration involves the complete freezing of the solution. Then, the frozen solution is partially thawed to recover a highly concentrated solution (Moreno et al., 2014a; Raventós et al., 2007; Sánchez et al., 2009). Block FC consists of three stages: initial freezing of the solution to form ice crystals, thawing, and recovering the solutes by controlled partial thawing (Moreno et al., 2014b; Moreno et al., 2013).

Solute loss in the formed ice crystal occurs in both block freeze concentration and falling-film freeze concentration. For falling-film FC, authors, such as Hernández et al. (2010), have suggested that one of the causes of solute loss is the formation of ice in the dendritic form, which tends to trap solutes. For block FC, authors, such as Okawa et al. (2009), Moreno et al. (2014a), Moreno et al. (2014b) and Petzold et al. (2013), have suggested that solute loss in block freeze concentration may be related to the structure of the ice formed during the process. Several authors have studied the formation of ice crystal structures in the crystallization process, which have been observed through various microscopic techniques, indicating that nucleation, growth, and ripening affect ice crystal morphology (Kiani and Sun, 2011; Otero et al., 2012; Petzold and Aguilera, 2009).

Additionally, the contributions of Goff et al. (2003) showed that applying heat treatments to aqueous frozen solutions can affect the presence of occlusions in the formed crystals. Hottot et al. (2007) studied the freeze-drying of pharmaceutical products and demonstrated the influence of various freezing process parameters on the structure and textural properties of the frozen materials. These authors proposed that a suitable annealing treatment might homogenize and greatly increase the sizes of ice crystals. Nakagawa et al. (2009) reported that the use of annealing in block freeze concentration might have a positive effect on solute recovery.

Annealing is the process of holding (or exposing) a crystal in a solution at a temperature below the melting point for a certain period (Kubota, 2011). This treatment is performed after the freezing stage by heating the sample above the glass transition temperature and keeping it at that temperature for a certain period (Hottot et al., 2007).

The application of these strategies in the block freeze-concentration process can affect solute recovery by modifying the solute recovery efficiency of the process. Consequently, the purpose of

this work was to study the effect of the heating temperature of the ice block (T_H) and the application of annealing (+, -) on the morphology of the ice and the solute yield during total block freeze-concentration of a coffee extract. Additionally, although some studies regarding crystal morphology using other microscopy techniques (Fan et al., 2015; Islam et al., 2015) have been reported, this work aimed to quantify the possible morphological changes that occur during annealing to explain the phenomenon through certain methodologies, such as image analysis. This technique consists of 5 basic steps, and although it has been widely used in various food matrices (Hernández-Carrión et al., 2015), to the best of our knowledge, only a few studies have applied it to ice crystal formation due to the level of difficulty in handling this type of sample.

2 Materials and Methods

2.1 Materials

Freeze-dried coffee from a single process batch, supplied by Buencafé Liofilizado de Colombia (Colombian Coffee Growers Federation, Colombia), was used to prepare the solutions. The coffee was dissolved in distilled water at 35 °C to obtain solutions with an initial concentration of 15% w/w, according to the protocol proposed by Moreno et al., (2014b). Samples were stored at 4 °C for 12 h.

2.2 Methods

Two sets of block freeze-concentration tests were performed with coffee solutions: one set studied the effect of the heating temperature and the application of annealing on the morphology of ice blocks obtained by freezing coffee solutions, and the other set studied the effect of the heating temperature and the application of annealing on solute recovery during freeze-concentration of coffee extracts.

2.2.1 Block Freeze Concentration Tests

FC Protocol

The freeze-concentration procedure was conducted with the total block technique using the equipment developed by Moreno et al. (2014b). The equipment consisted of a cylindrical container in which 160 g of the coffee solution to be freeze-concentrated was placed. The container possessed an inner and outer jacket that allowed circulation of the cooling and heating fluids (ethylene glycol/water, 53%, w/w). The cylindrical container measured 52.5 mm in diameter and 85 mm in height, and the internal jacket was 19 mm in diameter. Heat transfer occurred in a single direction, radially from the inner jacket of the equipment.

First, the coffee solutions were frozen. Then, the ice block was heated at temperatures below the freezing point or it was subjected to annealing, according to the experimental design. Finally, the ice block was thawed at a controlled temperature, and the concentrated solution was recovered. Sample temperatures were recorded at four equidistant points in the equipment using PT100 - IP65 sensors (Testo, Germany) with a measuring interval from -50 to 300 °C \pm 0.01 °C.

Experimental design

Two factors were studied during the tests: the heating temperature (T_H) and the application of annealing (A). The heating temperature was the temperature of the coolant of the internal jacket, which was below the freezing point ($T_H = -5$ and -10°C). The second factor was the application or non-application of annealing. The annealing application consisted of maintaining the sample at the heating temperature for 12 hours. A complete factorial design of two factors with two levels was used (2^2) so that a total of four (4) treatments performed. In addition, a freeze-concentration test without the ice block heating and annealing was used as a control (T5) (Moreno et al., 2014b). All of the treatments were conducted in triplicate. Table 1 shows the performed treatments.

The tests were performed during the freeze-concentration of coffee solutions, which involved four stages. First, the coffee solution was cooled to -20°C (freezing); then, the ice block was heated at the heating temperature ($T_H = -10^\circ\text{C}$ and -5°C); next, the sample was maintained at this temperature for 12 hours for the annealing test. Finally, the sample was cooled to -20°C (final cooling), ensuring that the temperature was constant at all points in the sample and at each temperature change in the protocol, as shown in Fig. 1.

2.2.2 Ice Crystal Morphology Tests

FC Protocol

The protocol described in section 2.2.1 was followed in treatments T1 to T4, evaluating the same factors and study levels. For this set of treatments, controlled thawing to separate solutes was not used.

Digital Image Acquisition

The samples of the formed ice blocks were taken at the end of the final cooling and before the thawing stage in each of the block freeze-concentration treatments, ensuring that the block temperature was -20°C at all times. This temperature was used to facilitate the ice cutting in the microtome without sample thawing.

Thick cuts measuring $60\ \mu\text{m}$ were created in directions parallel and perpendicular to the freezing front growth. Perpendicular cuts were created at 1.2, 3.6, 6.0, 8.4, and 11.1 mm from the cooling wall (the inner jacket of the container) in a Cryostat freezing microtome (Leica CM1850, Germany) at -20°C for each sample collected from the treatments.

These cuts were observed in a cooling chamber (INTEC HCS301i, USA) at -20°C . The chamber was fitted to the plate of the inverted microscope (Nikon Eclipse Ti, Japan) with a 10X objective in the bright field. Images of the ice crystals were captured using a digital camera (NIKON DIGITAL SIGHT DS-Fi1, Japan) attached to the microscope.

Image Segmentation

Digital images with a 1280 × 960 pixel resolution were processed and analysed using the image analysis software ImageJ (National Institute of Health, USA). These images were converted from grey scale (8-bits) to black and white format/binary images. Ice crystals were identified by adjusting the threshold to a range between 160 and 170 (Aguilera and Germain, 2007).

Digital Image Analysis

At least 150 crystals were manually identified for each group of images, ensuring a standard error of less than 8%.

According to Eq. 4, the following size morphometric parameters were determined: area, perimeter, and hydraulic diameter (HD). In addition, according to Eqs. 5 and 6, the following shape morphometric parameters were determined: circularity (Circ.) and aspect ratio (AR) (Igathinathane et al., 2008).

$$HD = 4A/P \quad (4)$$

$$Circ. = 4\pi A/(P)^2 \quad (5)$$

$$AR = a/b \quad (6)$$

Here, HD is the hydraulic diameter of the ice crystal, Circ. is the circularity of the ice crystal, AR is the aspect ratio of the ice crystal, A is the area of the ice crystal, P is the perimeter of the ice crystal, *a* is the major axis of the ice crystal, and *b* is the minor axis of the ice crystal (*a* ≥ *b*).

2.2.3 Data Analysis for solute recovery

The freeze-concentration tests for solute recovery analysis were developed by the protocol described in section 2.2.1., including a final thawing and separation stage. After the final cooling, the thawing stage for solute recovery was performed by heating the ice block from the external jacket of the equipment at 40 °C, as shown in Fig. 1. Ten (10) equal mass fractions were collected from the thawed solution, and the mass was measured on a scale (Ohaus PA3102, USA), equalling 3100 g ± 0.01 g. The concentrations of the fractions were measured by refractometry (Atago Pal 100, Japan). Solid concentrations were expressed as mass fractions of total solids (Xs), according to the equation reported by Moreno et al., (2015b). The following variables were calculated for data analysis:

Thawing Fraction (f): the ratio of the thawed liquid mass to the initial mass of the solution (Eq. 1) (Miyawaki et al., 2012; Nakagawa et al., 2010):

$$f = m_{liq}/m_0 \quad (1)$$

where f is the thawing fraction, m_{liq} is the thawed liquid mass, and m_0 is the initial mass of the solution.

Solute Recovery Yield (Y): the ratio of the mass of the solute recovered in the freeze-concentrated liquid fraction to the mass of the solute in the initial solution (Eq. 2) (Moreno et al., 2013; Nakagawa et al., 2010):

$$Y = m_{s\ liq} / m_{s\ 0} \quad (2)$$

where Y is the solute recovery yield, $m_{s\ liq}$ is the mass of the solute in the thawed liquid fraction, and $m_{s\ 0}$ is the mass of the solute in the initial solution.

Concentration Index (CI): the ratio of the solid fraction in the freeze-concentrated liquid to the solid fraction in the initial solution (Eq. 3) (Nakagawa et al., 2009):

$$CI = X_{s\ liq} / X_{s\ 0} \quad (3)$$

where CI is the concentration index, $X_{s\ liq}$ is the concentration of solids in the thawed liquid fraction, and $X_{s\ 0}$ is the concentration of solids in the initial solution.

Area under curve Y vs. f: The area under the curve was used to compare the treatments. The area under the curve was calculated from the Y vs. f graph and represents the cumulative amount of solute recovered during freeze-concentration. The area under the curve was used to compare the separation efficiency between treatments and to verify the influence of each studied factor. The larger the area, the greater the amount of solute recovered in a smaller thawing fraction (Moreno et al., 2014b).

The area under the Y vs. f curve of the treatments was obtained using the statistical software SAS 11.0 through a Spline regression procedure.

2.2.4 Changes in Ice Crystal Structure over Time

An ice crystal test to evaluate the morphology was performed during each FC step for the treatment with the best solute recovery results. The procedures for image analysis described in section 2.2.2 were applied at the end of the freezing stage (step 1), the ice block heating stage (step 2), the annealing stage (step 3), and the final cooling stage (step 4).

2.2.5 Statistical analysis

For the solute recovery tests, a response surface regression procedure was used to determine the effect of the heating temperature during the ice block heating and the effect of the application of

annealing on the area under the curve with a confidence interval of 95%. Analysis of variance (ANOVA) was applied to the results of the area under the curve followed by an LSD test with a significance level of 95%.

Analysis of variance (ANOVA) was applied to compare the results of the morphometric parameters. Tukey's honestly significance test was used to determine the significant differences between treatments at a fixed cutting distance and between cutting distances for a fixed treatment with a significance level of 95%.

3 Results and Discussion

3.1. Morphometric Characteristics of Ice Crystals

An example of the images obtained for the ice morphology treatments in the perpendicular and parallel cuts is presented in Fig 2. The characteristic morphology of ice crystals obtained from the perpendicular cuts can be observed in Fig. 2 (A), showing a disk crystal structure similar to that found by Petzold and Aguilera, 2009 (Petzold and Aguilera, 2009) with water and sucrose solutions. In Fig. 2, ice crystals appear white, and the freeze-concentrated phase appears dark brown.

The crystals observed in cuts parallel to the freezing front growth (Fig.2 (B)) showed continuous growth as they moved away from the cooling wall (inner jacket), creating larger channels than the image size (incomplete crystals). This was similar to the results observed in other tests, such as those performed by Farhangdoust et al. (Farhangdoust et al., 2013).

Cuts created perpendicular to the freezing front growth in the block for each treatment (Fig. 3) showed an increase in crystal size as the freezing front growth advanced. This result was statistically significant, as shown in Fig 4A and can be explained because the heat transfer rate was lower when the freezing front growth advanced. It is well known that ice size is strongly dependent on the freezing condition (Pardo et al. 2002). This effect allowed the formation of small ice crystals after nucleation (near the freezing wall) and increased crystal growth as the freezing front growth advanced.

Additionally, for treatments T1 and T3 (which had the application of annealing), larger sizes of the formed crystals were observed, possibly because the presence of annealing allowed more growth of ice crystal due to certain phenomena, such as Ostwald ripening (Nakagawa et al., 2006; Nakagawa et al., 2009). The change that occurred in the morphology of the ice crystals may have caused a thickening of the area where the freeze-concentrated solution was located. This produced a better route to recover the solutes contained in the initially formed solid matrix (Nakagawa et al., 2010).

Processing and analysis of the acquired images were performed to obtain morphometric parameters that provide information about how the ice crystal morphologies of each treatment were formed. Fig. 4 (A, B) shows the average area and the hydraulic diameter of the ice crystals.

Crystal size growth was observed as the freezing front growth advanced, obtaining an average area of 0.0243 mm² at 1.2 mm and 0.0830 mm² at 11.1 mm for treatment T1, 0.0051 mm² and 0.0700 mm² for treatment T2, 0.0107 mm² and 0.0893 mm² for treatment T3, and 0.0089 mm² and 0.0565 mm² for treatment T4, respectively.

Additionally, for each cut created in the block, treatment T1 ($T_H = -5^\circ\text{C}$ and annealing) showed a significantly higher average area and hydraulic diameter than the other treatments, and treatment T3 ($T = -10^\circ\text{C}$ and annealing) showed a larger crystal size in three of the five cuts compared with treatments T2 and T4, which did not include the application of annealing.

Fig. 5 (A) shows the average circularity of the ice crystals. As observed, treatment T1 had a significantly higher circularity than the other treatments in the first four cuts, with values ranging from 0.46 to 0.60. On the other hand, T3 showed the same circularity as T2 and T4. This result indicates that annealing modified the circularity only when it was performed at -5°C . In general, the circularity was not modified significantly with the cut distance.

Fig. 5 (B) shows the average aspect ratio of the ice crystals. These results showed an inverse behaviour in relation to circularity. A greater circularity produced a lower aspect ratio, and the lowest values for each of the cuts were obtained for treatment T1 ($T_H = -5^\circ\text{C}$ and +), which ranged from 1.96 to 3.45. The only treatment with a statistically significant difference for the aspect ratio was T1, indicating that annealing modified the aspect ratio only when it was performed at -5°C .

According to the evaluated morphometric parameters, it was clear that as the freezing front growth advanced in the block, the diameter and the area of the ice crystals increased and its circularity and aspect ratio were not significantly different. This indicates that the freezing rate did not modify the ice circularity as much as the size. However, only T1 showed significantly different morphometric parameters. This showed that annealing applied at -5°C modified the structures of the ice crystals formed during block freeze-concentration, and this affected the solute recovery. Other authors have been reported that ice morphology changes during long-term preservation (Sung-Hee et al., 2006; Hagiwara et al., 2005).

Considering the behaviour displayed by the crystalline structures in the perpendicular and parallel cuts to the freezing front growth in the block, a diagram showing ice crystal growth in the freeze-concentrator was proposed to observe the possible tortuosity that the concentrated liquid phase must supply at the stage of separation. A graphical representation was developed using the diameter measurements obtained in the morphometric characterization of the ice at each of the distances. The ice crystal model is shown in Fig. 6. Ice crystals in the perpendicular direction to the freezing front growth are smaller because they are closer to the cooling wall, and their size increases as heat transfer occurs from the outer radius to the inner radius of the freeze-concentrator.

3.2. Effect of heating temperature and annealing application on solute recovery

Block freeze-concentration tests were performed to obtain the thawing fractions of the evaluated treatments. Fig. 7 shows the results of the concentration indexes (a) and solute recovery yields (b) for each thawing fraction. These graphs show a behaviour consistent with that reported in the literature (Moreno et al., 2014b).

The CI vs. f curves (Fig. 7A) show that CI is greater than 1 in the first fractions, indicating that most of the solute was recovered. Therefore, the first samples were freeze-concentrated. Treatment T1 reached a CI maximum of 1.4 in $f=0.3$, achieving a concentration 1.4 times greater than the initial concentration in the third recovered fraction. The CI maximum for the other treatments was approximately 1.2, revealing that the solute recovery during T1 was more efficient. Then, applying annealing at high temperatures increases the amount of solute recovered. The CI behaviour was nearly the same in treatments T2, T3, and T4 but at lower CI values.

In Fig. 7(A), the horizontal line at $CI=1$ corresponds to the moment when the thawing stage must be stopped to avoid diluting the sample and to recover the greatest possible amount of solids (Moreno et al., 2014b). For treatment T1, 74.4% of the coffee solids were recovered in $f=0.6$, showing a more efficient recovery than in the other treatments with values when $f=0.6$ of 67.2% for T2, 68.1% for T3, and 67.6% for T4.

In Fig. 7(B), the area under the curve is the integral of the function Y vs. f . The area value is bound between 0, when the solutes are not recovered, and 1, when all the solute is recovered. The diagonal line shows the situation in which the thawed liquid fraction has the same concentration as the initial solution; in this case, there is no FC. The greater the area under the curve, the greater the amount of recovered solute at a given f . In this work, similar to the results of IC, the Y vs f curves (Fig. 7B) showed that treatment T1 had a higher solute recovery than treatments T2, T3, and T4.

Treatment T1 ($T_H=-5^{\circ}\text{C}$ and annealing) showed the highest area under the curve and concentration index. The same treatment showed a significantly higher ice crystal area and significantly higher ice crystal circularity than the other treatments. These results indicate that annealing at high temperatures increased the crystal size and circularity, consequently increasing the solute recovery in block freeze-concentration. Several authors have reported that the ice morphology strongly affects solute recovery in block freeze-concentration (Yee et al., 2003; Nakagawa et al., 2009).

The results obtained for T1 may be explained by the diffusion of solutes during the thawing stage. The application of annealing at -5°C induced a modification in the ice structure and facilitated the concentration of the solution. That is, if the ice crystal shape was close to a circular shape, then recovering a greater solid concentration in block freeze-concentration will be possible. This may be

because this crystal geometry favours the creation of a less tortuous structure, which favours the escape of the freeze-concentrated solution from the ice matrix, thus facilitating solute recovery, as shown in Fig 6. This result confirms what was mentioned by Nakagawa et al., (2010).

Comparing the results obtained from the treatments during the T5 test, which was performed under the same conditions but without ice block heating and annealing, CI showed a similar behaviour to treatments T2, T3 and T4 with a CI maximum of 1.2 obtained in the first four fractions (Moreno et al., 2014b). Additionally, 17% more solute was recovered at the CI maximum during treatment T1, which indicated that annealing had a positive effect on improving the recovery efficiency in block freeze-concentration. This effect may be due to morphological changes that may have occurred in the ice crystal, providing a greater solute recovery at a lower f .

The results of the average Y vs. f area under the curve of the FC tests and the T5 control test (Table 2) showed that treatment T1 had the greatest area under the curve, thus, the highest solute recovery for block freeze-concentration with a value of 0.686. Therefore, it is clear that the application of annealing at the highest temperature led to a greater recovery than that found in treatments T2, T3, and T4, which did not show a significant difference ($\alpha=0.05$) relative to test T5. Annealing at -10°C did not show a significant effect on the area under the curve, possibly because of the morphology of the ice crystal.

The results obtained from the response surface regression analysis performed to determine the significance of the main and combined effects on the Y vs. f area under the curve are shown in Table 3.

The effect of the application of annealing and the combined effect of the heating temperature and annealing were found to significantly affect the area under the curve for the intervals studied. These effects had a positive correlation with the obtained area under the curve; therefore, increasing the values of these variables will increase the solute recovery in freeze-concentration. This could indicate that certain phenomena occurred during the isothermal hold of the sample, such as Ostwald ripening, which is time-dependent (Pronk et al., 2005). These phenomena modify the crystalline structure, which can affect solute recovery (Nakagawa et al., 2009).

The ice crystal images for treatments T1 and T4, obtained by performing a crosscut at 6.0 mm in the block (Fig. 6), showed changes in the crystal structure. The morphologies of the ice crystals changed in terms of size and circularity when subjected to $T_H=-5^{\circ}\text{C}$ and the application of annealing, which had the highest solute recovery. The increased size and circularity of the ice crystals in T1 also showed a thickening of the channels where the freeze-concentrated solution was located, resulting in lower tortuosity in the crystal structure and facilitating solute recovery during thawing (Fig. 6A). This allowed the concentrated liquid in the concentration stage to have a better solute recovery, a higher concentration index, and a smaller thawing fraction, as evidenced by the solute recovery results (Fig. 7A).

3.3. Changes in ice crystal structure over time

Changes in ice crystal structure over time were evaluated for T1 at 6.00 mm in the ice block obtained in the freeze-concentrator (Fig. 8) because this treatment showed the most representative values in the morphometric parameters evaluated and an improved recovery of solutes.

Fig. 8 shows the points of the ice crystal morphology that changed during each stage in treatment T1. As observed, small, elongated, irregular ice crystals were formed during stage 1, which may be due to the freezing rate used to freeze the solution. In stage 2, the first change in crystal morphology occurred when the temperature during the ice block heating was increased to -5 °C, at which a change in the shape and size of the crystal was observed, possibly because the increased temperature allowed an increase in mass transfer that promoted crystal growth. In stage 3, a change in the shape and an increase in the size of the crystals was observed when the annealing was applied at -5 °C. This may be due to Ostwald ripening, which involves adherence of the small ice crystals to the larger ones, causing the crystal size to increase and the crystal quantity to decrease (Hartel, 2002; Petzold and Aguilera, 2009; Pronk et al., 2005). Stage 4 showed the final structures of the crystals when the temperature was decreased to -20°C after annealing, which increased the crystal size compared with the first stage of the treatment.

Table 4 contains the morphometric parameters calculated for each step evaluated in treatment T1, showing an increase in size when the sample was subjected to annealing, a change in shape as the annealing progressed, and an increase in circularity, thus showing a decrease in aspect ratio.

4 Conclusions

The analysis of ice crystal morphology revealed that annealing at -5 °C during block freeze-concentration modified the crystalline structure, producing more circular crystals with larger sizes, which generated less tortuous channels for the subsequent recovery of the concentrated solution. Under these conditions, the best solute recovery was obtained. Ice crystal sizes were also shown to increase as the freezing front growth advanced in the ice block. The application of annealing and the combination of the heating temperature and annealing significantly affected the ice morphology, consequently increasing the solute recovery in block freeze-concentration. Thus, annealing may be a useful strategy to increase the concentration efficiency in block freeze-concentration.

Acknowledgements

This research was funded by the Universidad de La Sabana and COLCIENCIAS through project 1230521-28461, 2011. The authors would like to thank Engineer Carlos Eduardo Osorio of Buencafé Liofilizado de Colombia for supplying the coffee used for testing. The authors would like to thank María Fernanda Quiroz and Edgar Cao of the Universidad de La Sabana for the loan and useful advice regarding the cryostat freezing microtome. The authors would like to thank Adriana

Ortega of the Sanitas Lab Technology for providing microscopy supplies and Prof. Pedro Urbano for assistance with model sketching. The author C.M. Robles would like to thank the Universidad de La Sabana for providing the graduate assistantship for her studies in the Master of Design and Process Management program. The author F.L. Moreno would like to thank COLCIENCIAS for the grant awarded for his doctoral studies (2013).

5 References

- Aguilera, J. M., & Germain, J. C. (2007). 10 - Advances in image analysis for the study of food microstructure. In *Understanding and Controlling the Microstructure of Complex Foods* (pp. 261–287). Woodhead Publishing Series in Food Science, Technology and Nutrition. <http://doi.org/10.1533/9781845693671.2.261>
- Belén, F., Sánchez, J., Hernández, E., Auleda, J. M., & Raventós, M. (2012). One option for the management of wastewater from tofu production: Freeze concentration in a falling-film system. *Journal of Food Engineering*, 110(3), 364–373.
- Fan, Y., Zhu, J., Yan, S., Chen, X., & Yin, J. (2015). Nucleating effect and crystal morphology controlling based on binary phase behavior between organic nucleating agent and poly(l-lactic acid). *Polymer*, 67, 63–71.
- Farhangdoust, S., Zamanian, a., Yasaei, M., & Khorami, M. (2013). The effect of processing parameters and solid concentration on the mechanical and microstructural properties of freeze-casted macroporous hydroxyapatite scaffolds. *Materials Science and Engineering: C*, 33(1), 453–460.
- Fissore, D., Pisano, R., & Barresi, A. a. (2014). Applying quality-by-design to develop a coffee freeze-drying process. *Journal of Food Engineering*, 123, 179–187.
- Goff, H. ., Verespej, E., & Jermann, D. (2003). Glass transitions in frozen sucrose solutions are influenced by solute inclusions within ice crystals. *Thermochimica Acta*, 399(1-2), 43–55.
- Hagiwara T., Mao J., Suzuki T., Takai R., 2005. Ice recrystallization in sucrose solutions store in a temperature range of -21°C to -50°C. *Food Science and Technology Research*, 11, (4), 407-411.
- Hartel, R. W. (2002). 13 - Crystallization in foods. In *Handbook of Industrial Crystallization* (pp. 287–304).
- Hernández-Carrión, M., Hernando, I., Sotelo-Díaz, I., Quintanilla-Carvajal, M.X. & Quiles, A. (2015). Use of image analysis to evaluate the effect of high hydrostatic pressure and pasteurization as preservation treatments on the microstructure of red sweet pepper. *Innovative Food Science and Emerging Technologies*, 27, 69-78.

- 481 Hernández, E., Raventós, M., Auleda, J. M., & Ibarz, a. (2010). Freeze concentration of must in a
482 pilot plant falling film cryoconcentrator. *Innovative Food Science & Emerging Technologies*,
483 11(1), 130–136.
- 484 Hottot, A., Vessot, S., & Andrieu, J. (2007). Freeze drying of pharmaceuticals in vials: Influence of
485 freezing protocol and sample configuration on ice morphology and freeze-dried cake texture.
486 *Chemical Engineering and Processing: Process Intensification*, 46(7), 666–674.
- 487 Igathinathane, C., Pordesimo, L. O., Columbus, E. P., Batchelor, W. D., & Methuku, S. R. (2008).
488 Shape identification and particles size distribution from basic shape parameters using ImageJ.
489 *Computers and Electronics in Agriculture*, 63(2), 168–182.
- 490 Islam, M. N., Zhang, M., Fang, Z., & Sun, J. (2015). Direct contact ultrasound assisted freezing of
491 mushroom (*Agaricus bisporus*): growth and size distribution of ice crystals. *International*
492 *Journal of Refrigeration*.
- 493 Kiani, H., & Sun, D.-W. (2011). Water crystallization and its importance to freezing of foods: A
494 review. *Trends in Food Science & Technology*, 22(8), 407–426.
- 495 Kubota, N. (2011). Effects of cooling rate, annealing time and biological antifreeze concentration
496 on thermal hysteresis reading. *Cryobiology*, 63(3), 198–209.
- 497 Miyawaki, O., Kato, S., & Watabe, K. (2012). Yield improvement in progressive freeze-
498 concentration by partial melting of ice. *Journal of Food Engineering*, 108(3), 377–382.
- 499 Miyawaki, O., Liu, L., Shirai, Y., Sakashita, S., & Kagitani, K. (2005). Tubular ice system for scale-up
500 of progressive freeze-concentration. *Journal of Food Engineering*, 69(1), 107–113.
- 501 Moreno, F. L., Quintanilla-Carvajal, M. X., Sotelo, L. I., Osorio, C., Raventós, M., Hernández, E., &
502 Ruiz, Y. (2015a). Volatile compounds, sensory quality and ice morphology in falling-film and
503 block freeze concentration of coffee extract. *Journal of Food Engineering*, 166, 64–71.
- 504 Moreno, F. L., Raventós, M., Hernández, E., & Ruiz, Y. (2014a). Behaviour of falling-film freeze
505 concentration of coffee extract. *Journal of Food Engineering*, 141, 20–26.
- 506 Moreno, F. L., Raventós, M., Hernández, E., & Ruiz, Y. (2014b). Block freeze-concentration of
507 coffee extract: Effect of freezing and thawing stages on solute recovery and bioactive
508 compounds. *Journal of Food Engineering*, 120, 158–166.
- 509 Moreno, F. L., Raventós, M., Hernández, E., Santamaría, N., Acosta, J., Pirachican, O., Torres L., &
510 Ruiz, Y. (2015b). Rheological Behaviour, Freezing Curve, and Density of Coffee Solutions at
511 Temperatures Close to Freezing. *International Journal of Food Properties*, 18(2), 426–438.
- 512 Moreno, F. L., Robles, C. M., Sarmiento, Z., Ruiz, Y., & Pardo, J. M. (2013). Effect of separation and
513 thawing mode on block freeze-concentration of coffee brews. *Food and Bioproducts*
514 *Processing*, 91, 396–402.

- 515 Nakagawa, K., Hottot, A., Vessot, S., & Andrieu, J. (2006). Influence of controlled nucleation by
 516 ultrasounds on ice morphology of frozen formulations for pharmaceutical proteins freeze-
 517 drying. *Chemical Engineering and Processing: Process Intensification*, 45(9), 783–791.
- 518 Nakagawa, K., Maebashi, S., & Maeda, K. (2009). Concentration of aqueous dye solution by
 519 freezing and thawing. *The Canadian Journal of Chemical Engineering*, 87(5), 779–787.
- 520 Nakagawa, K., Maebashi, S., & Maeda, K. (2010). Freeze-thawing as a path to concentrate aqueous
 521 solution. *Separation and Purification Technology*, 73(3), 403–408.
 522 <http://doi.org/10.1016/j.seppur.2010.04.031>
- 523 Okawa, S., Ito, T., & Saito, A. (2009). Effect of crystal orientation on freeze concentration of
 524 solutions. *International Journal of Refrigeration*, 32(2), 246–252.
- 525 Otero, L., Sanz, P., Guignon, B., & Sanz, P. D. (2012). Pressure-shift nucleation: A potential tool for
 526 freeze concentration of fluid foods. *Innovative Food Science & Emerging Technologies*, 13,
 527 86–99. <http://doi.org/10.1016/j.ifset.2011.11.003>
- 528 Pardo, J.M., Suess, F., Niranjana, K., 2002. An investigation into the relationship between freezing
 529 rate and mean ice crystal size of coffee extracts. *Trans IChemE* 80, 176–182.
- 530 Petzold, G., & Aguilera, J. M. (2009). Ice Morphology: Fundamentals and Technological
 531 Applications in Foods. *Food Biophysics*, 4(4), 378–396.
- 532 Petzold, G., Niranjana, K., & Aguilera, J. M. (2013). Vacuum-assisted freeze concentration of sucrose
 533 solutions. *Journal of Food Engineering*, 115(3), 357–361.
- 534 Pronk, P., Hansen, T. M., Ferreira, C. a. I., & Witkamp, G. J. (2005). Time-dependent behavior of
 535 different ice slurries during storage. *International Journal of Refrigeration*, 28(1), 27–36.
- 536 Raventós, M., Hernández, E., Auleda, J., & Ibarz, A. (2007). Concentration of aqueous sugar
 537 solutions in a multi-plate cryoconcentrator. *Journal of Food Engineering*, 79(2), 577–585.
- 538 Sánchez, J., Ruiz, Y., Auleda, J. M., Hernandez, E., & Raventós, M. (2009). Review. Freeze
 539 Concentration in the Fruit Juices Industry. *Food Science and Technology International*, 15(4),
 540 303–315.
- 541 Sung-Hee P., Jee-Yeon K., Geun-Pyo H., Hae-Soo K. and Sang-Gi M., 2006. Effect of Ice
 542 Recrystallization on Freeze Concentration of milk Solutes in a Lab-Scale Unit. *Food Science*
 543 *Biotechnology*. 15, 196-201.
- 544 Van Pelt, W. H. J. M., & Bassoli, D. G. (1990). Freeze concentration: coffee-product and economic
 545 analysis. *Café, Cacao, Thé*, 34(1), 37–45. Retrieved from
 546 <http://cat.inist.fr/?aModele=afficheN&cpsidt=19244315>

Yee P.L., Wakisaka M., Shirai Y., Hassan M.A., 2003. Effects of Single food components on freeze
concentración by freezing and thawing technique. Japan Journal of Food Engineering, 4, 77-
82.

Highlights

- Crystal morphology was affected by annealing in the block freeze-concentration of coffee extracts.
- Applying annealing at high temperatures increases the amount of solute recovered during the block freeze-concentration of coffee extracts.

Fig. 1. Diagram of the annealing protocol for treatment T1.

Fig. 2 Description of ice crystals (10X). (A.) Ice crystal structure in a cut perpendicular to the freezing front growth. (B.) Ice crystal structure in a cut parallel to the freezing front growth.

Fig. 3. Structure of the ice crystals observed in each treatment at 10X in the direction perpendicular to the freezing front growth.

Fig. 4. Morphometric parameters evaluated in the cuts created for each test. (A). Area, (B). Hydraulic diameter. Treatments with the same letter do not differ significantly.

Fig. 5. Morphometric parameters evaluated in the cuts created for each test. (A). Circularity and (B). Aspect ratio. Treatments with the same letter do not differ significantly.

Fig. 6. Representation of the possible arrangement of the ice crystal obtained in the block freeze-concentrator. Ice crystals for cuts perpendicular to the freezing front growth of the treatments with the highest and lowest circularity. (A). T1 ($T_H = -5^\circ\text{C}$; +) and (B). T4 ($T_H = -10^\circ\text{C}$; -).

Fig. 7. (A). Concentration index (CI) as a function of the coffee thawing fraction and (B). Solute recovery yield as a function of the coffee thawing fraction. T1 (\square): $T_A = -5^\circ\text{C}$ and $t = 12$ h, T2 (\circ): $T_A = -5^\circ\text{C}$ and $t = 0$ h, T3 (\diamond): $T_A = -10^\circ\text{C}$ and $t = 12$ h, T4 (\triangle): $T_A = -10^\circ\text{C}$ and $t = 0$ h and T5 (\times): First cooling - control test (Moreno et al., 2014b).

Fig. 8. Images obtained at 10X in the four stages of treatment T1 at 6.00 mm in the freeze-concentrated ice block. (A). Step 1: freezing, (B). Step 2: heating at T_H , (C). Step 3: annealing, (D). Step 4: cooling.

Table 1. Experimental design and control treatment

Test	T _H	Application of Annealing (A)
T1	-5	+
T2	-5	-
T3	-10	+
T4	-10	-
T5*	-	-

(+) with annealing (-) without annealing. * A freeze-concentration test without block heating and annealing were used as a control (Moreno et al., 2014b).

Table 2. Y vs. f area under the curve values of FC tests and the T5 control test (Moreno et al., 2014b).

Test	T _H	A	Area under curve	CI at f=0.6	CI max
T1	-5	+	0.686 ^a	1.05	1.39
T2	-5	-	0.635 ^b	1.10	1.15
T3	-10	+	0.650 ^b	1.05	1.18
T4	-10	-	0.640 ^b	1.13	1.18
T5	-	-	0.640 ^b	1.11	1.18

Different letters indicate statistically significant differences ($p < 0.05$).

Table 3. Significance of the main and combined effects of the tests.

Parameter	Standard estimator	Pr > t
Intercept	0.630	> 0.0001
T_H	-0.001	0.4645
PA	0.008	0.0002*
$T_H \cdot T_H$	0	-
PA · T_H	0.001	0.0021*
PA PA	0	-

* statistically significant ($P < 0.05$).

Table 4. Morphometric parameters of crystals 6 mm in the ice block after freeze concentration.

	Step 1	Step 2	Step 3	Step4
Area (mm²)	0.038 ± 0.001 ^a	0.042 ± 0.001 ^{a, b}	0.062 ± 0.002 ^c	0.046 ± 0.001 ^b
Hydraulic Diameter (mm)	0,123 ± 0.009 ^c	0,143 ± 0.009 ^d	0,192 ± 0.010 ^e	0,180 ± 0.007 ^f
Circularity	0.328 ± 0.005 ^g	0.408 ± 0.007 ^h	0.490 ± 0.008 ⁱ	0.582 ± 0.007 ^j
Aspect Ratio	5.738 ± 0.114 ^k	4.447 ± 0,106 ^l	3.238 ± 0,071 ^m	2.238 ± 0,049 ⁿ

Different letters indicate statistically significant differences ($p < 0.05$).

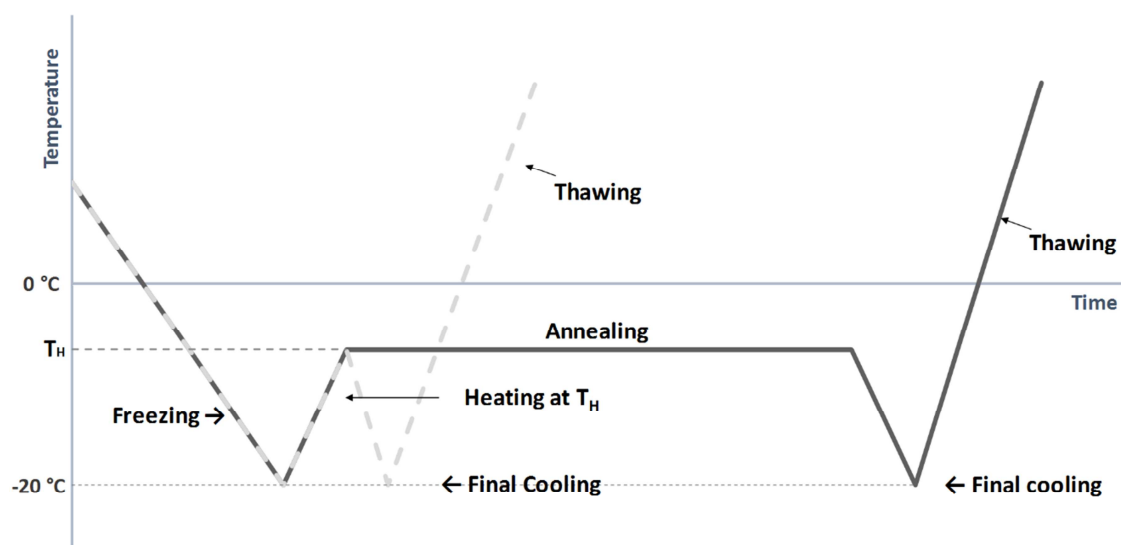


Fig. 1. Diagram of the annealing protocol. —Treatment with annealing, --- Treatment without annealing.

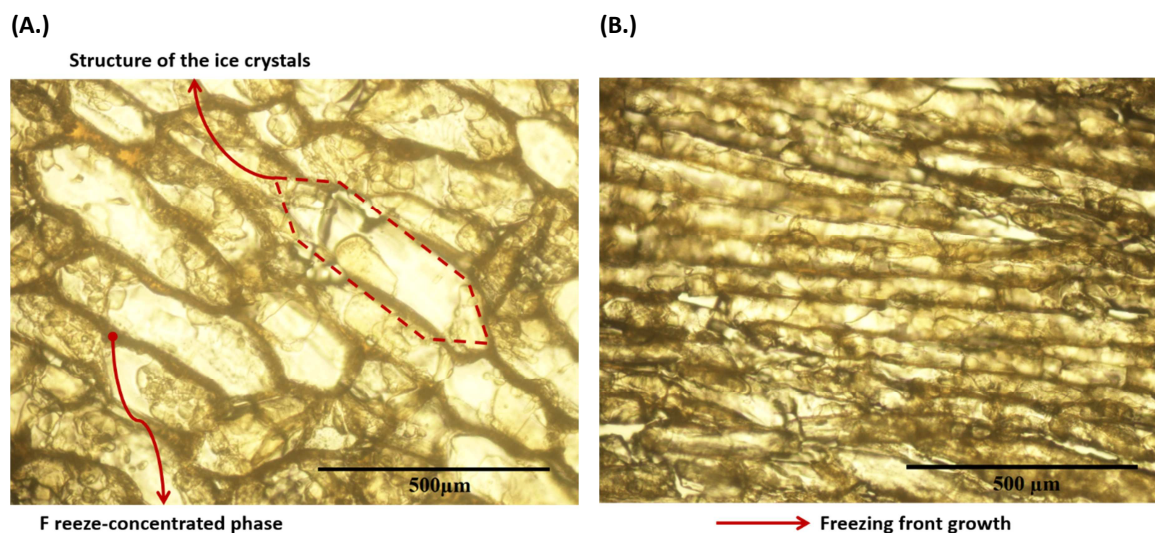


Fig. 2 Description of ice crystals (10X). (A.) Ice crystal structure in a cut perpendicular to the freezing front growth. (B.) Ice crystal structure in a cut parallel to the freezing front growth.

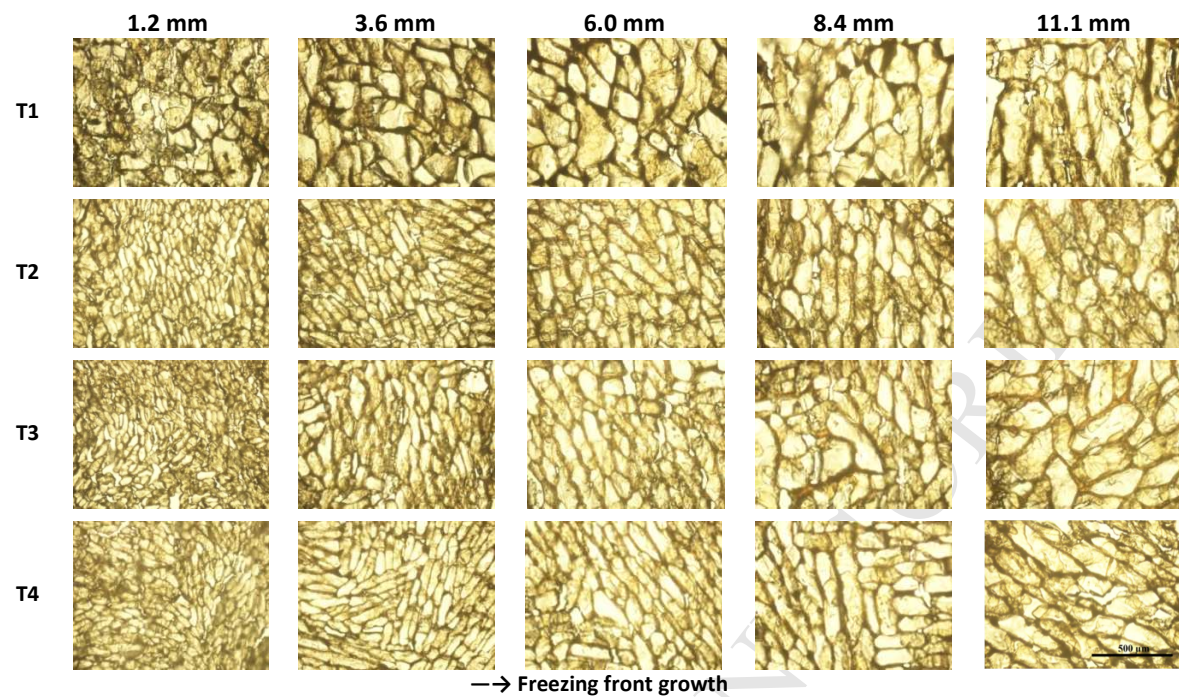
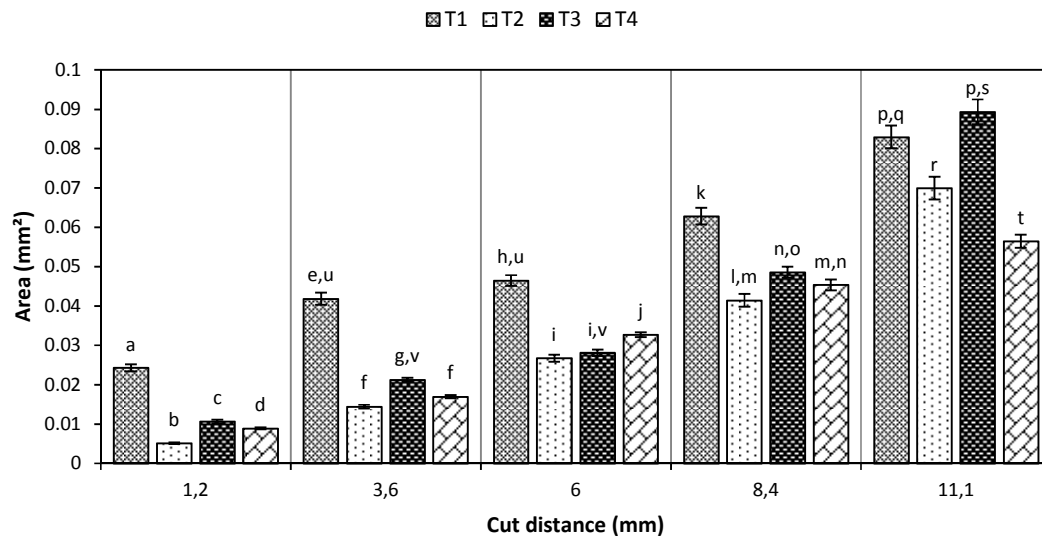


Fig. 3. Structure of the ice crystals observed in each treatment at 10X in the direction perpendicular to the freezing front growth.

(A.)



(B.)

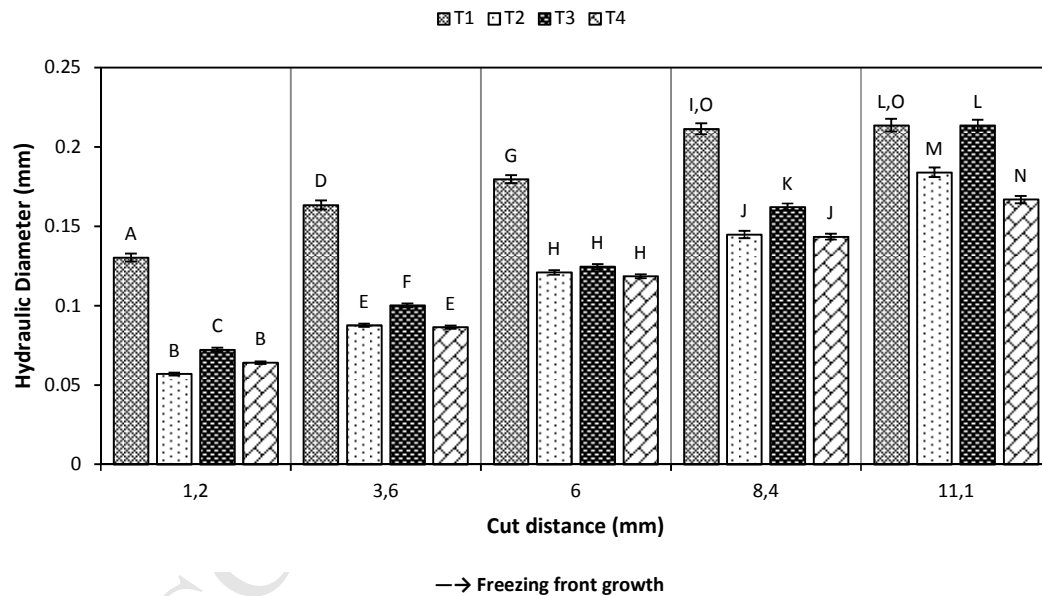
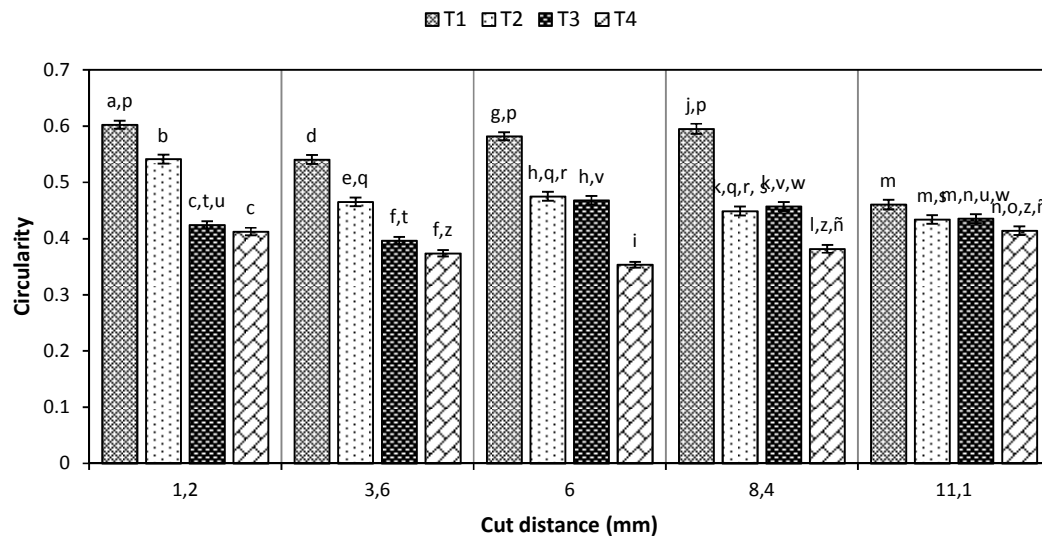


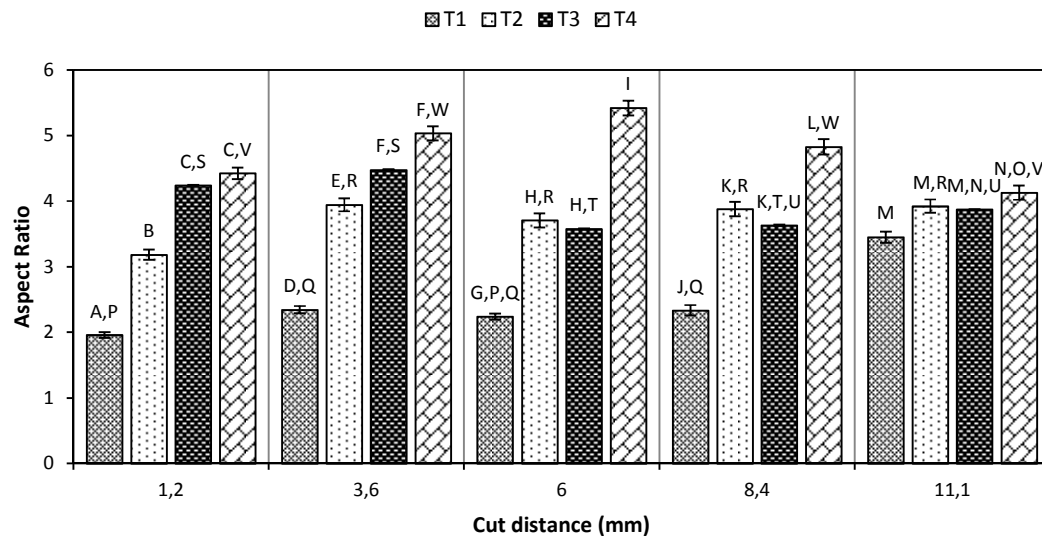
Fig. 4. Morphometric parameters evaluated in the cuts created for each test. (A). Area, (B). Hydraulic diameter. Treatments with the same letter do not differ significantly.

(A.)



→ Freezing front growth

(B.)



→ Freezing front growth

Fig. 5. Morphometric parameters evaluated in the cuts created for each test. (A). Circularity and (B). Aspect ratio. Treatments with the same letter do not differ significantly.

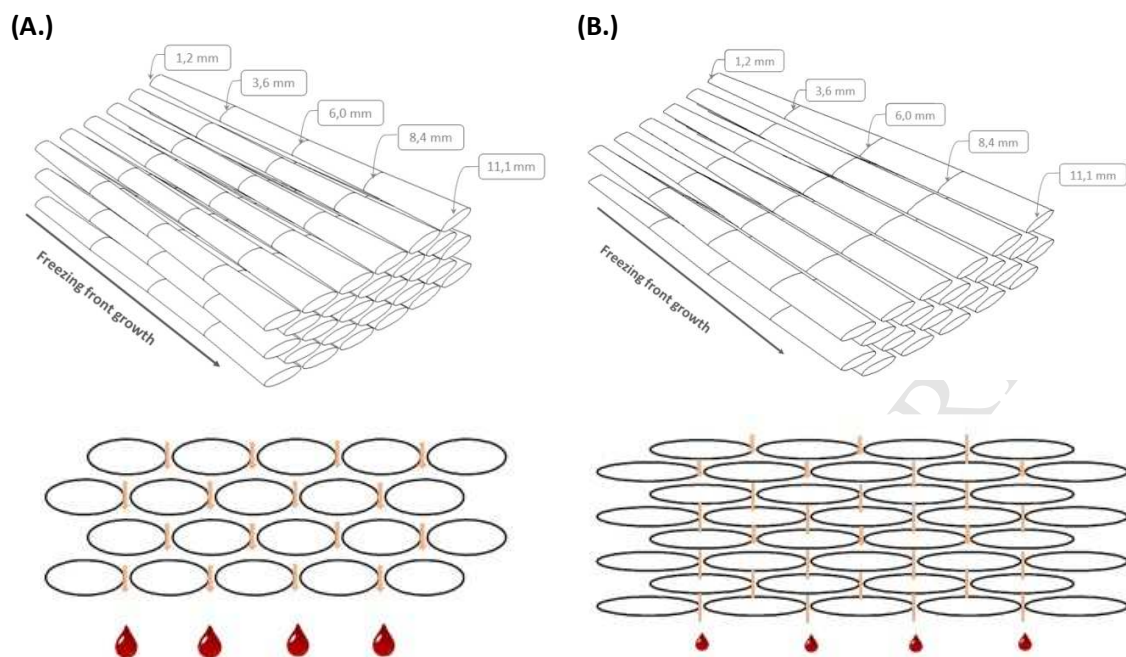


Fig. 6. Representation of the possible arrangement of the ice crystal obtained in the block freeze-concentrator. Ice crystals for cuts perpendicular to the freezing front growth of the treatments with the highest and lowest circularity. (A). T1 ($T_H = -5^\circ\text{C}$; +) and (B). T4 ($T_H = -10^\circ\text{C}$; -).

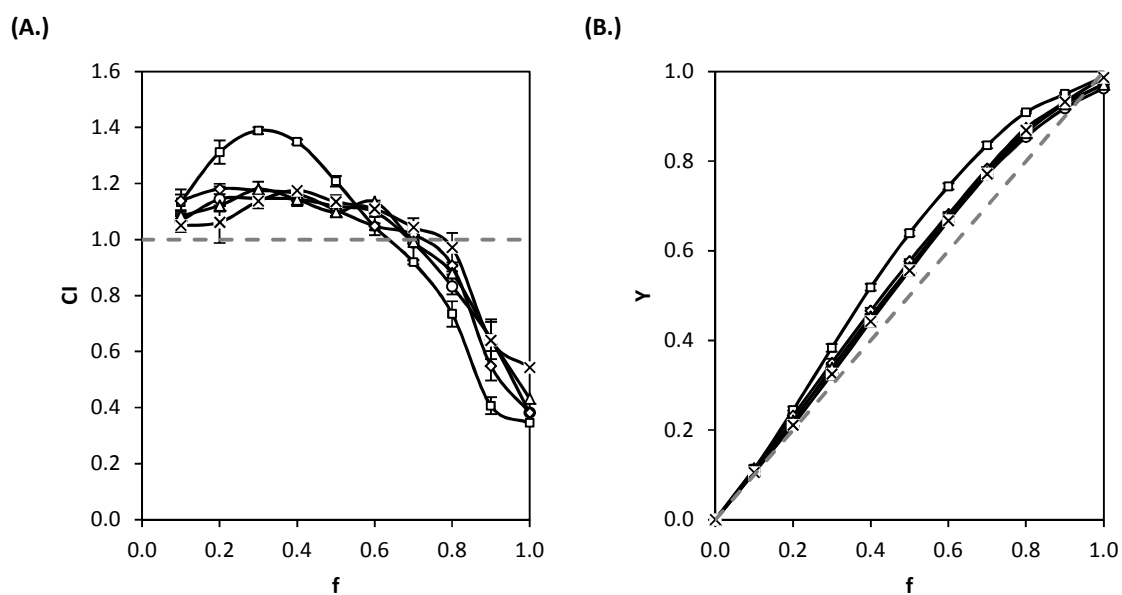


Fig. 7. (A). Concentration index (CI) as a function of the coffee thawing fraction and (B). Solute recovery yield as a function of the coffee thawing fraction. T1 (\square): $T_H = -5^\circ\text{C}$ and +; T2 (\circ): $T_H = -5^\circ\text{C}$ and -; T3 (\diamond): $T_H = -10^\circ\text{C}$ and +; T4 (\triangle): $T_H = -10^\circ\text{C}$ and -; and T5 (\times): First cooling - control test (Moreno et al., 2014b).

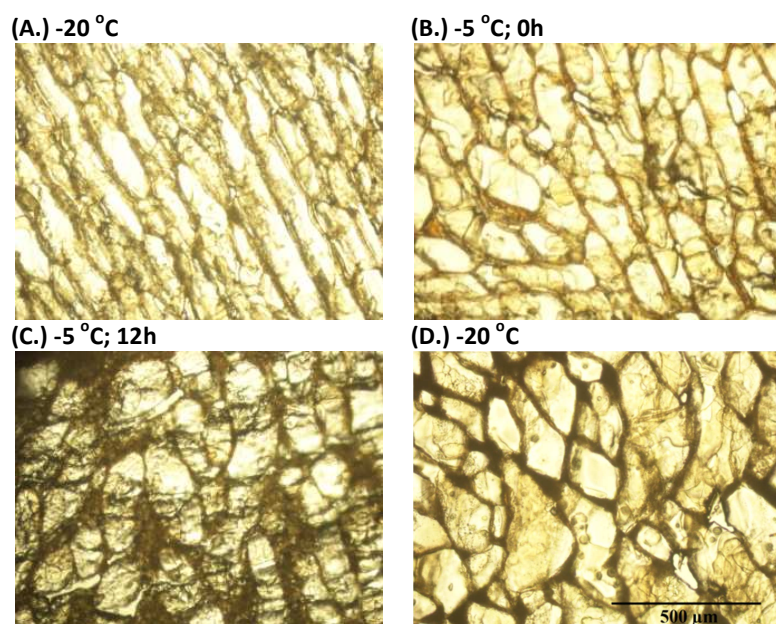


Fig. 8. Images obtained at 10X in the four stages of treatment T1 at 6.00 mm in the freeze-concentrated ice block. (A). Step 1: freezing, (B). Step 2: heating at T_H , (C). Step 3: annealing, (D). Step 4: cooling